Universität Rostock Traditio et Innovatio

Construction of an Experimental Setup for Pulsed Wire Discharge Experiments

Pre-thesis by Max Bigelmayr

at

the Chair of High Voltage and High Current Technology HHT

Prof. Dr.-Ing. Dirk Uhrlandt

under the supervision of Petrus Pieterse

Contents

1. Introduction and motivation

Pulsed wire discharge (PWD) experiments have a long tradition in different disciplines, since the invention of the Leyden jar in 1745. Edward Nairne first discharged capacitors through metal wires [1], which resulted in a rapid vaporisation of the metal, combined with the creation of a shock wave. Despite the slow heating process which was well known from low voltages that caused wires to glow, a high voltage discharge through a metal wire is characterised by a rise in high current dI/dt, which not only allows the wire to melt but also vaporises the metal [2]. Before the first invention of storage oscilloscopes in 1946 by the US company Tektronix, it was impossible to measure the electrical discharge behavior of capacitors through metal wires. In the 1960's and 1970's many scientists performed pulsed wire discharge experiments in order to do research within plasma physics, high speed forming of sheet metals through *Hydrosparc Forming* as well as other technological processes [3].

In 1965 Frank Früngel published the book "High Speed Pulse Technology" [4] in which he describes the different methods of measurement and diagnosis as for example through X-Ray photography, in order to analyse the interesting phenomena of pulsed wire discharges. Since those days the typical time segments which occur during the phenomena are well known. However even today they are not fully understood. In the past high expectations were placed on the application of shockwave creation by exploding wires, but in practical use such setups e.g. for sheet metal forming appeared to be too large and bulky [5]. Nevertheless, the technology behind high voltage capacitors has improved considerably within the last decades. New foil as well as dielectric materials offer us now the ability to produce high energy density capacitors of up to 3.0J/cm^3 [6]. This technical advancement, from an economic stand point, could pave the way in regards to the use of capacitor driven applications in combination with exploding wires, in order to produce shockwaves. Since the efficiency of diverse setups concerning *underwater electrical wire explosions* (*UEWE*s) depends on many different parameters, e.g. the capacitor voltage, circuit inductance, wire material and dimensions, a detailed understanding of the dependencies and mechanisms involved is essential.
Presented within this report is the creation of an experimental setup, for the purpose of analysing pulsed wire discharge experiments. After familiarising the reader with the basic theoretical principles, the main aspects of the experimental setup will be explained in detail. Therefore special emphasis was placed on the construction of a discharge chamber, a clamp device to attach the wires as well as on measurement techniques so as to be able to capture the voltage and current curves which occur during the discharges. In the final chapter of this report a first experiment with a X12CrNi18-8 steel wire is introduced and briefly mentioned.

2. The theory behind pulsed wire discharges

2.1. Types of discharge behavior

After charging a capacitor bank up to a predefined high voltage, the capacitor network is discharged through a metal wire [4] via a switching spark gap, ignitron or thyratron. Depending on the size, the capacitor bank usually contains several high voltage capacitors, which are connected to one another in parallel or series. However, this schematic setup can be simplified so as to solely contain a circuit with a capacitance C, a switch, an circuit inductance L, a time dependent wire resistance $R_W(t)$ and a constant circuit resistance R (Fig. 1).

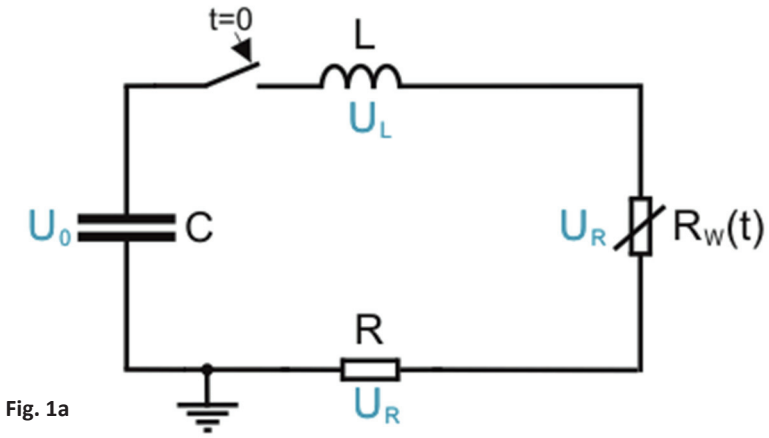

Fig. 1a

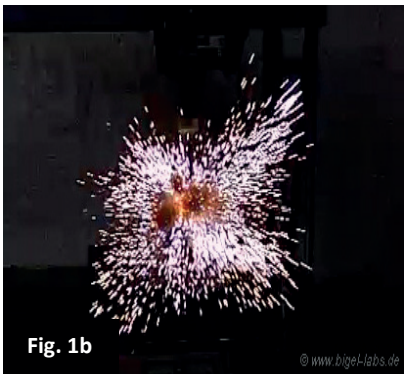

Fig. 1b

Fig. 1a: Schematic setup of pulsed wire discharge experiments: *a high voltage capacitor C is charged up to a certain voltage and discharged afterwards through a thin metal wire with a resistance $R_W(t)$. Due to the high current density the metal wire melts and vaporizes violently within a few microseconds.* ***Fig. 1b:*** **High speed photograph of an exploding wire**

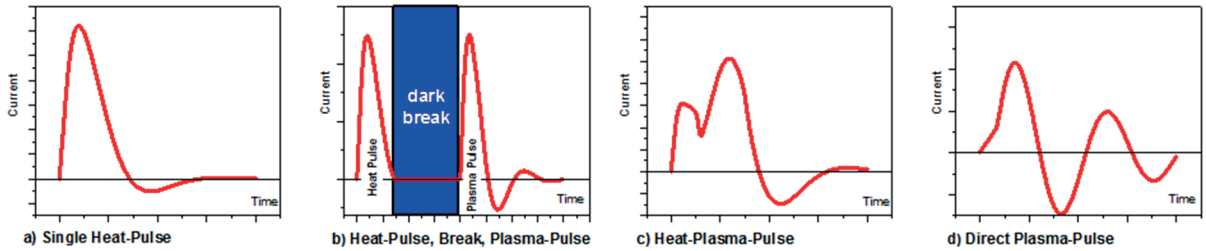

Fig. 2: Different types of discharge current behavior during pulsed wire discharges *(qualitative presentation)*

Depending on the discharge parameters (capacitance, voltage, inductance, wire material and dimensions) one is able to distinguish four different types of current curves I(t), which are shown in Fig. 2.

When a High Voltage Capacitor is discharged through a wire with large mass, the capacitors energy may not be adequate to vaporise the metal [7]. In this case the discharge curve is characterised by only a single pulse with one individual peak of current (Fig. 2a).

Depending on the capacitors energy and the given wire dimensions a second pulse of current (Fig. 2b) is able to occur after a so-called *Dark Break* [8]. Following the first heat pulse the resistance of the wire increases due to its temperature dependency. When the thermodynamic circumstances allow the appearance of boiling nuclei a second plasma pulse occurs, which surrounds the wire in the shape of a cylindric coat. In general, these secondary discharges oscillate due to the low resistance of the gas plasma from the metal vapor.

It is common that during experiments with thin wires (especially when the stored energy within the capacitor is larger than the wires enthalpy of vaporisation), the heat pulse and plasma pulse "melt together" with no Dark Break in between the two (Fig. 2c).

By using very thin or short wires the heat pulse (Fig. 2a) is not visible anymore within the graph (Fig. 2d). In this case, solely a direct discharge plasma occurs as a current of damped oscillation.

2.2 The theory behind CLR circuits

2.2.1 Differential equations and solutions to different types of discharge

As aforementioned the curves of current, which occur as a result of capacitors discharging, depend on the dimensions of the used wire. Diverse wire sizes cause different values to emerge concerning the implemented wires initial resistance. In order to better understand pulsed wire discharges and the exploding wire phenomena, it is useful to first of all comprehend the discharge behavior of a capacitor through a constant resistance R as well as a fixed circuit inductance L (CLR circuit). However the discharge of a charged capacitor through a constant resistance is similar to a circuit with an exploding wire. The examination of CLR circuits could help to improve and understand experiments with exploding wires.

The differential equations of a CLR circuit can be solved analytically for all three kinds of damp behavior. According to Kirchhoff's second law, the capacitor voltage U_C, inductance voltage U_L and resistor voltage U_R is:

$$U_C(t) + U_L(t) + U_R(t) = 0 \tag{2.1}$$

When expressing the occurring voltages through the current I(t), capacitance C, circuit inductance L and resistance R one is able to deduce the differential equation for the current:

$$\frac{1}{C} I(t) + L\frac{d^2I(t)}{dt^2} + R\frac{dI(t)}{dt} = 0 \tag{2.2}$$

Depending on the implemented resistance R one can distinguish three different types of discharge:

$$I(t) = \begin{cases} \dfrac{U_0}{2L\sqrt{\delta^2 - \omega_o^2}}\left(e^{-\delta+\sqrt{\delta^2-\omega_o^2}t} - e^{-\delta-\sqrt{\delta^2-\omega_o^2}t}\right) & R > 2\sqrt{\dfrac{L}{C}} \quad \text{(a)} \\ \dfrac{U_0}{L} te^{-\delta t} & R = 2\sqrt{\dfrac{L}{C}} \quad \text{(b)} \\ \dfrac{U_0}{L}\sqrt{\omega_o^2 - \delta^2}e^{-\delta t}\sin\sqrt{\omega_o^2 - \delta^2}t & R < 2\sqrt{\dfrac{L}{C}} \quad \text{(c)} \end{cases} \tag{2.3}$$

The first equation (2.3a) describes an overdamped circuit, the second (2.3b) a critically damped circuit and the last one an oscillating circuit which is underdamped (2.3c). A more detailed deduction of these equations is shown in [9]. The relationship between the angular frequency w_0 and the damping factor δ can be formulated in the following way:

$$\omega_0^2 = \frac{1}{LC} \qquad \delta = \frac{R}{2L} \tag{2.4}$$

The requirement for critical damping is given when

$$\omega_0^2 = \delta^2 \quad \Rightarrow \quad R = 2\sqrt{\frac{L}{C}} \tag{2.5}$$

counts, which can facilitate the approximation of the ideal average wire resistance.

2.2.2 The energy absorption within the resistor

Since the amplitude of a shock wave, that is produced by an exploding wire, depends on the speed at which a capacitors energy E_C is converted into heat energy within the given resistor, it is useful to deduce an expression regarding the absorbed energy inside the resistor $E_R(t)$. As the occurring discharge current during an exploding wire experiment is similar to that of an oscillating and a critically damped circuit, the expression $E_R(t)$ of these different situations below, is of particular interest.

Through analytical integration the energy absorption in the swing case (2.3c) occurs as:

$$E_R(t) = \int_0^t I^2(t)Rdt = RU^2 e^{(-2\delta t)} \frac{\delta\sqrt{(\omega^2-\delta^2)}\sin\left(2t\sqrt{(\omega^2-\delta^2)}\right) - \delta^2\cos\left(2t\sqrt{(\omega^2-\delta^2)}\right) + e^{(2\delta t)}(\delta-\omega)(\delta+\omega)+\omega^2\Big)}{4\delta L^2\omega^2(\delta-\omega)(\delta+\omega)} \qquad (2.6)$$

Regarding long periods of time all the stored energy from the capacitor is transformed into heat energy within the resistor:

$$E_{sum} = \lim_{t\to\infty}\left[RU^2 e^{(-2\delta t)} \frac{\left(\delta\sqrt{(\omega^2-\delta^2)}\sin\left(2t\sqrt{(\omega^2-\delta^2)}\right) + \left(\delta^2\left(-\cos\left(2t\sqrt{(\omega^2-\delta^2)}\right)\right) + e^{(2\delta t)}(\delta-\omega)(\delta+\omega)+\omega^2\right)\right)}{4\delta L^2\omega^2(\delta-\omega)(\delta+\omega)}\right] = \qquad (2.7)$$

$$= \frac{RU^2[(\delta-\omega)(\delta+\omega)]}{4\delta L^2\omega^2(\delta-\omega)(\delta+\omega)} = \frac{RU^2}{4\delta L^2\omega^2} = \frac{U^2C}{2}$$

Through curve sketching of the equation (2.3b) one is capable of showing in the critically damped circuit case, that the maximum discharge current is as follows:

$$I_{max} = -\frac{U_0}{L\delta}e^{-1} = -\frac{2U_0}{R_{APGF}}e^{-1} \approx 0,736\frac{U_0}{R_{APGF}} = 0,368U_0\sqrt{\frac{C}{L}} \qquad (2.8)$$

The equation below is provided by integration of $I^2(t)R$ within the damped circuit and represents the total energy absorbed by the resistor:

$$E_R(t) = U_0^2\left\{0,5C - e^{-\frac{2t}{\sqrt{LC}}}\left[\frac{t^2}{L} + \sqrt{\frac{C}{L}}t + 0,5C\right]\right\} \qquad (2.9)$$

For long durations of time $t\to\infty$ the absorbed energy within the resistor becomes $0.5CU_0^2$ which is the value of the total stored energy inside the capacitor, prior to the discharge pulse. The value $E_R(t)$ within a critically damped circuit is always greater[1] compared to $E_R(t)$ in an underdamped or overdamped circuit. This is a very important phenomenon in regards to considerations concerning energy conversion during pulsed wire discharge experiments. Equation (2.9) provides an overview for any CLR circuit, as to how fast the energy stored in a capacitor is capable of being transformed into the resistor.

[1] Nevertheless for long times $E_R(t=\infty)$ converges to the same value $0.5CU_0^2$ for any kind of damping.

By utilising the equation (2.3) in combination with (2.9) the energy transformation process of CLR circuits can be calculated in order to receive a rough estimation of how a similar exploding wire discharge could look like. Fig. 3 below shows the discharge current and capacitor voltage for a CLR circuit with a capacitance of C=147µF, capacitor voltage of U=6kV, line inductance of L=9.0uH and a resistance of R=0.495Ω. The inherent energy distribution curves of a CLR circuit containing the just mentioned parameters are shown in Fig. 4 below.

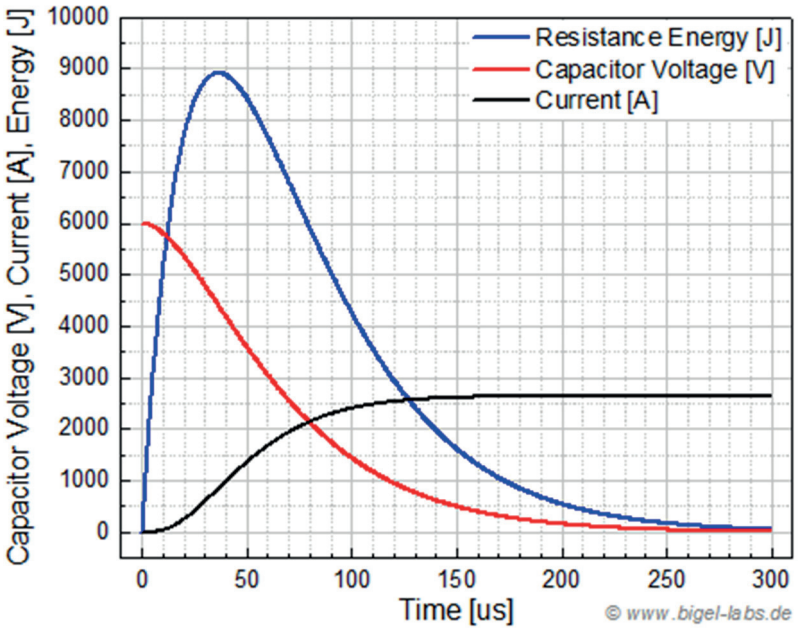

Fig. 3: A critically damped CLR circle (C=147µF, U=6kV, 9µH). *The discharge current (blue) was calculated with the equation (2.3b) and reaches a maximum value of nearly 9kA (in comparison to with equation (2.8)). The capacitor voltage (red curve) shows no reversal of voltage.*

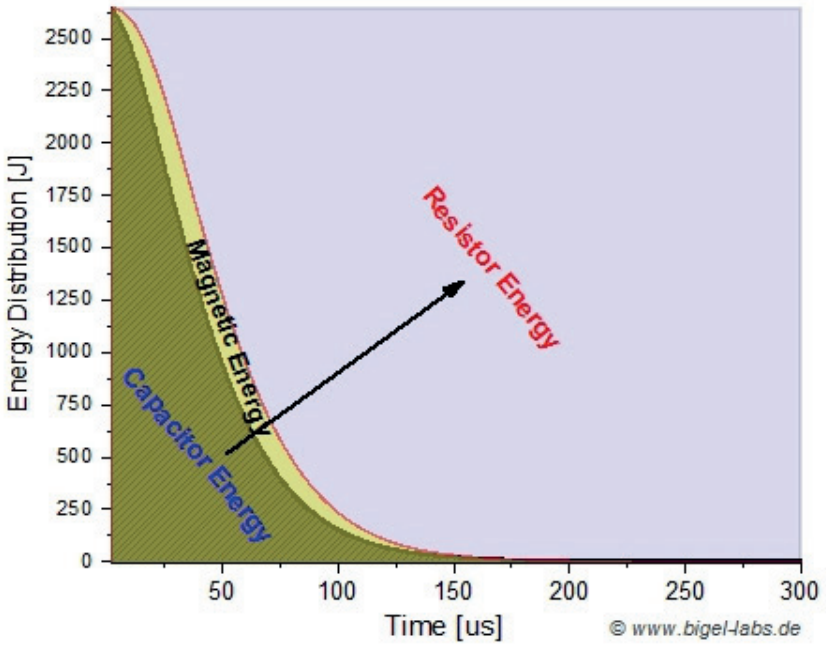

Fig. 4: Energy flux diagram: *The energy flux which occurs during a pulse discharge is split into the Capacitor Energy* $E_C(t) = \frac{1}{2}CU_C^2$, Magnetic Energy $E_L(t) = \frac{1}{2}LI^2(t)$ *and* Resistor Energy $E_R(t)$*. On the whole it is convenient to reduce L, this is done in order to attain a faster conversion of the stored capacitor energy into the resistor.*

2.3 The theory of discharge and pulsed wires

Up until now the CLR circuits viewed above depending on the absorbed energy, had a constant resistor R with no alteration of conductance. In practice the wire is vaporised by a capacitor discharge which changes its own resistance R_w during the occurrence of a pulse. Therefore, the variation in regards to the electrical resistivity ρ of a wire, must also be taken into consideration throughout experiments with pulsed wire discharges (Fig. 5).

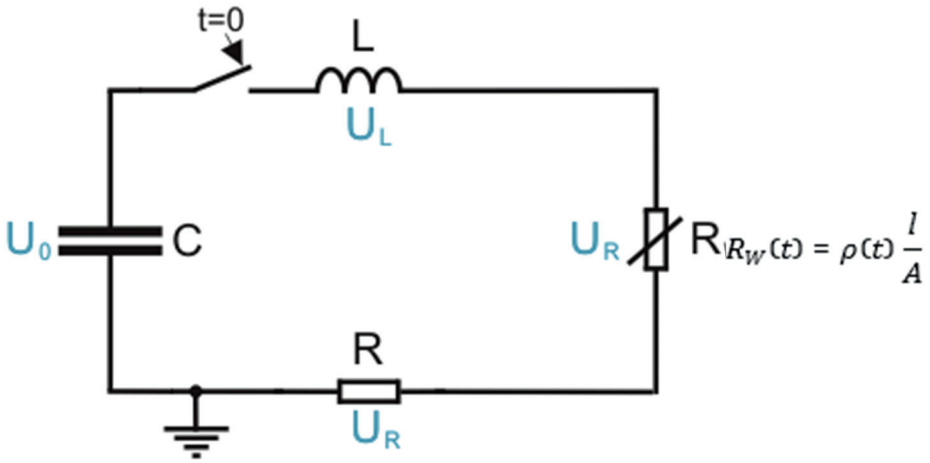

Fig. 5: Schematic of a CLR(t) circuit. *The given capacitor is discharged through a circle with a constant inductance L as well as a resistor R. The wire contains a resistance $R_W(t)$ which is temperature dependent, that is able to be modeled by a defined resistivity behavior ρ(t).*

When assuming a constant line resistance R and a variable wire resistance $R_w(t)$, Kirchhoff's second law states the following:

$$U_C(t) + U_L(t) + U_R(t) + U_W(t) = 0 \qquad (2.10)$$

Here the current is incorporated into the differential equation:

$$\frac{1}{C} I(t) + L\frac{d^2I(t)}{dt^2} + \frac{dI(t)}{dt}\left(R + R_W(t)\right) + I(t)\frac{dR_W(t)}{dt} = 0 \qquad (2.11)$$

Through second derivation in respect to time one receives:

$$\frac{d^2I(t)}{dt^2} = -\frac{1}{L}\left(\frac{1}{C} I(t) + \frac{dR_W(t)}{dt} I(t) + \left(R + R_W(t)\right)\cdot\frac{dI(t)}{dt}\right) \qquad (2.12)$$

The time dependent resistance of a wire with the length l and cross section A can be approximated as follows:

$$R_W(t) = \rho(t)\frac{l}{A} \qquad (2.13)$$

To solve this differential equation the electrical resistivity ρ(t) can be expressed as a linearised function, which depends on the absorbed energy density $\rho_E(t)$ within the given wire.

3. The experimental setup

3.1 The capacitor bank network and circuit diagram

In order to be able to perform pulsed wire discharge experiments, a capacitor bank network was built (Fig. 6). The entire setup contains two different types of capacitor bank: a basic capacitor bank (KB1) with a capacitance of C_{KB1}=50µF and an additional capacitor bank (KB2) with a capacitance of C_{KB2}=100µF. The networks total capacitance lies at 150µF and its energy storage is 2700J, when charged up to 6000V (Fig. 7).

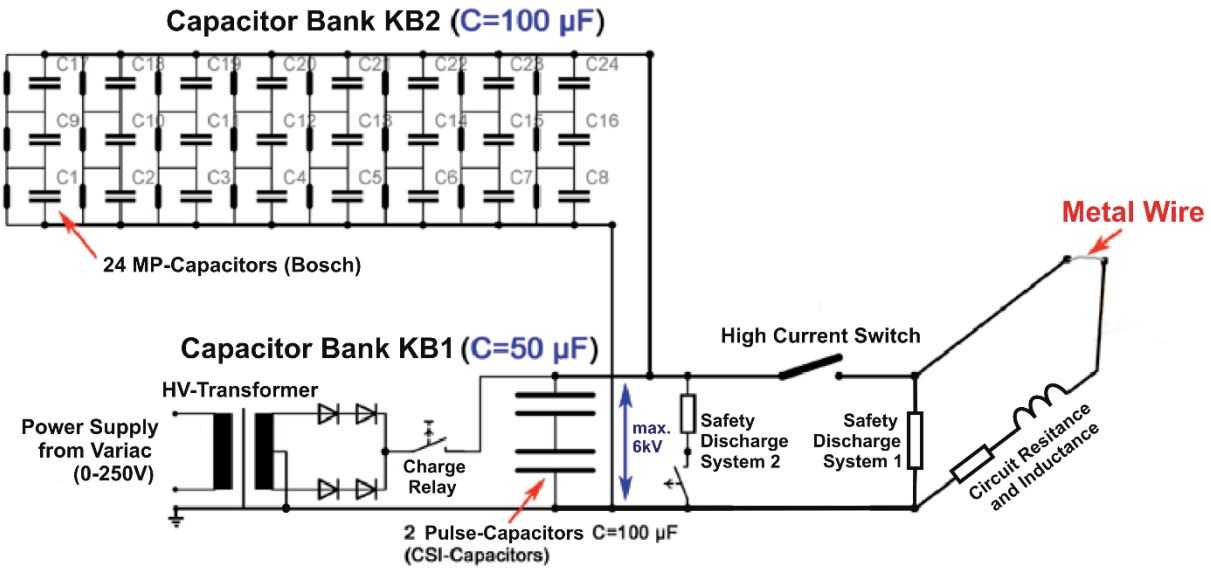

Fig. 6: Circuit diagram of the whole capacitor bank

The basic capacitor bank system contains a charge circuit with a so-called *Oil Burner Ignition Transformer* (OBIT), which provides a peak output voltage of around 6.2kV. The two high voltage outputs are rectified and then brought together. Over a high voltage reed relay (charge relay) the two capacitor banks are able to be charged up to a maximum voltage of 6.2kV. The input voltage of the transformer is able to be controlled by a variac transformer which supplies the HV-transformer with electricity from a safe distance. After reaching a certain voltage, which lies between 1000V and 6000V, the charge circuit is switched off by a charge relay. Then the discharge switch is triggered by a pneumatic system, which allows a totally safe firing of the system. The discharge current is conducted through a high voltage coaxial cable (RG164U) to the plasma chamber (Fig. 8, ⑤), which allows for a low inductance energy transformation (compare chapter 2.2.2). Inside the massively constructed chamber, wires of a length of up to 250mm are able to be attached onto a special clamp device (chapter 3.2.2). The discharge current returns within the outer shell of the coaxial cable back to the device, where an additional inductance (Fig. 8, ⑦) can be mounted if so required. Over a coaxial shunt resistor (Fig. 8, ⑨), the discharge current is measured and stored by a digital oscilloscope. When one activates the *High Current Switch,* the energy of the capacitor is also distributed throughout the *Safety Discharge System 1* (Fig. 8, ④). This Safety Discharge System 1 contains 12 ceramic resistors from Rosenthal (GK19.5x120, 2.5kOhm, U_{max}=1600V), which are connected to one another in series. With a total resistance of 30kΩ, the decay constant τ provides: RC=30kΩ·150µF=4.5s. When one compares this value with the time constant of the circuit containing a metal wire (T≈200µs), the loss of energy during the pulse discharge dissipation in the safety discharge system 1 is neglectable. Nevertheless,

dangerous charges of high voltage inside the capacitor bank are capable of dissipating after 6τ=27s, so as to be left with safe voltage values (U_C<15V), even in the event of no metal wire being placed between the electrodes within the discharge chamber.

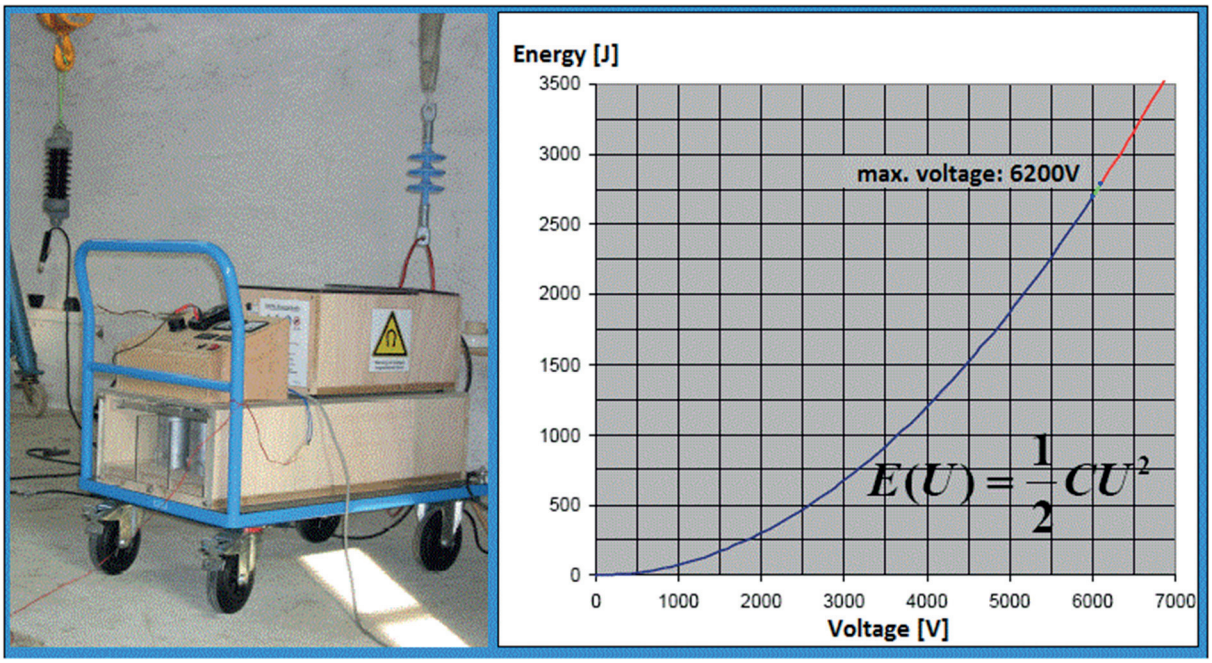

Fig. 7: An energy diagram from the capacitor bank

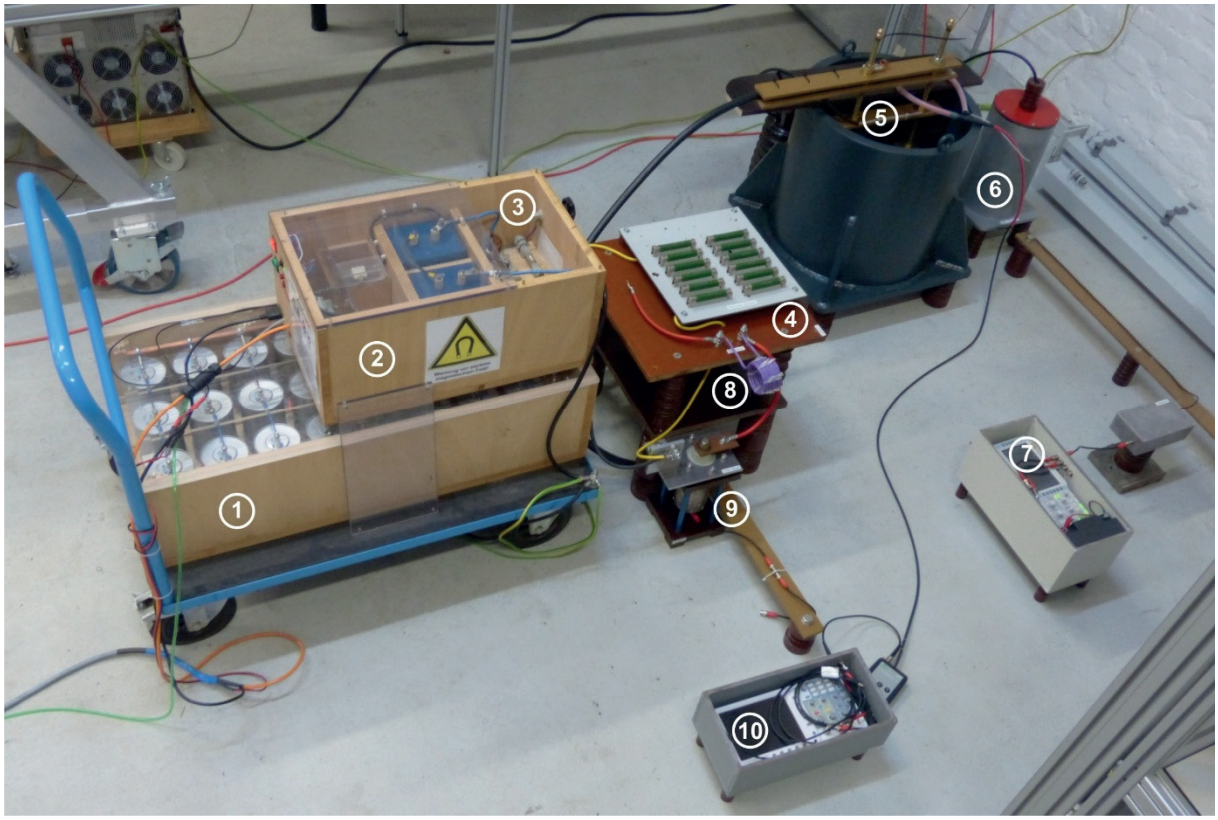

Fig. 8: Experimental setup: *① capacitor bank KB2, ② capacitor Bank KB1, ③ high current switch, ④ safety discharge system 1, ⑤ discharge chamber with metal wire, ⑥ high voltage divider, ⑦ digital storage oscillosope nr. 2, ⑧ variable inductance L*, *⑨ coaxial shunt resistor, ⑩ digital storage oscillosope nr. 1*

3.2 The concept and construction of a discharge chamber

3.2.1 The discharge chamber

The construction of the vaporisation chamber is made of massive steel (30mm thick, type 235JR) and sites on high voltage isolators. In order to discover the ideal geometry required, different CAD-models (Fig. 9a) were constructed digitally. Afterwards the geometries were imported into *ANSYS Explicit Dynamics STR* so as to be able to simulate the stability during shockwaves. In order to account for this different high explosive charges were placed in the middle inside the virtual chamber in order to be able to identify the weakest point of the construction (Fig. 9b). In future experiments it should also be possible to do pulsed discharges underwater with an energy of up to several 100kJ, so as to be able to create underwater shock waves, without the risk of damaging the chamber.

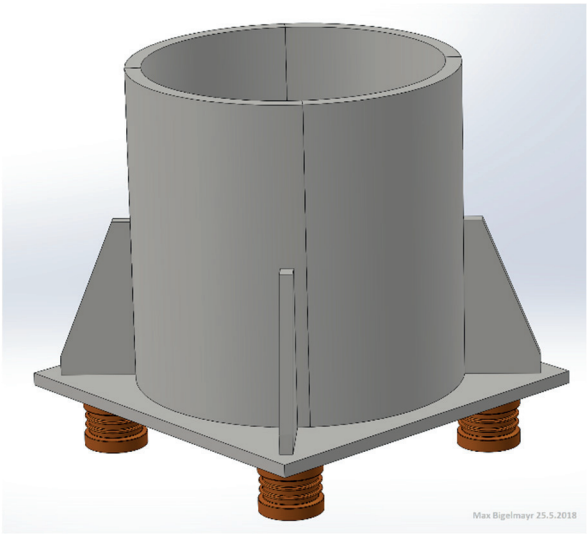

Fig. 9a: CAD-model of the discharge chamber

Different dimensions of 235JR steel were designed and compared by thickness, stability and weight.

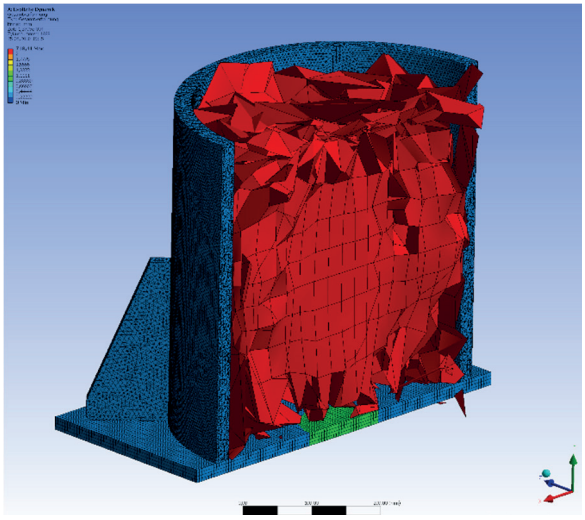

Fig. 9b: Shockwave simulation: *A virtual charge of 100 grams of plastic explosive was placed inside and in the middle of the discharge chamber. Via numerical simulations in ANSYS Explicit Dynamics STR an ideal geometry and size for the chamber was attained.*

After completing the CAD models, all the needed individual parts where converted into STEP data files and then cut by laser into the required shapes. The main pipe was ordered from a large steel trader as saw cut. The pipe was MAG-welded together with the bottom plate and supporting angles in three layers (Fig. 10a). The assembled and brushed construction was then varnished with a so called *Fitter Coating* (Fig. 10b).

Fig. 10a: MAG-welded chamber

Fig. 10b: Coated chamber post welding and brushing

3.2.2 The construction of the clamp device

Because strong shock waves are produced by the exploding wires inside the discharge chamber, a solid construction had to be built in order to be able to clamp down the wire threads. The steel assembly had to be electrically isolated from the discharge chamber and was realised to allow any kind of simple attachment of one or two coaxial cables in parallel (RG164U or RG218U), which supply the experiment from the capacitor bank. Furthermore, it should be possible to clamp down wires of a length of up to 250mm (diameter 100µm-1000µm) between two electrodes. The distance of these electrodes should be adjustable within the range of 0-250mm, without having to change the center line once it is fastened by the clamp device, in regards to the currents path. This guarantees for a nearly constant inductance value regarding the clamp device and also nearly completely elevates the dependency of wire length. After taking all these requirements into consideration, a CAD model of a clamp device was built (Fig. 11). The central conductor of the high voltage cable RG164U which runs away from the capacitor bank is fastened to a threaded M16 rod at the place Ⓐ, while the outer conductor is attached to another threaded M16 rod at the place of Ⓕ. The threaded rods are fixed in place by massive terminals made of brass at the places Ⓒ and Ⓓ. Within each of these terminals a horizontally drilled hole was milled, they each allow a single threaded M16 metal rode to be place through them. These two threaded rods act as electrodes with a variable distance, between which a wire is able to be attached between them. Halfway between Ⓐ-Ⓒ and Ⓕ-Ⓓ an RG213U coaxial cable is put in place so as to be able to measure the decline in voltage between the place Ⓑ and Ⓔ.

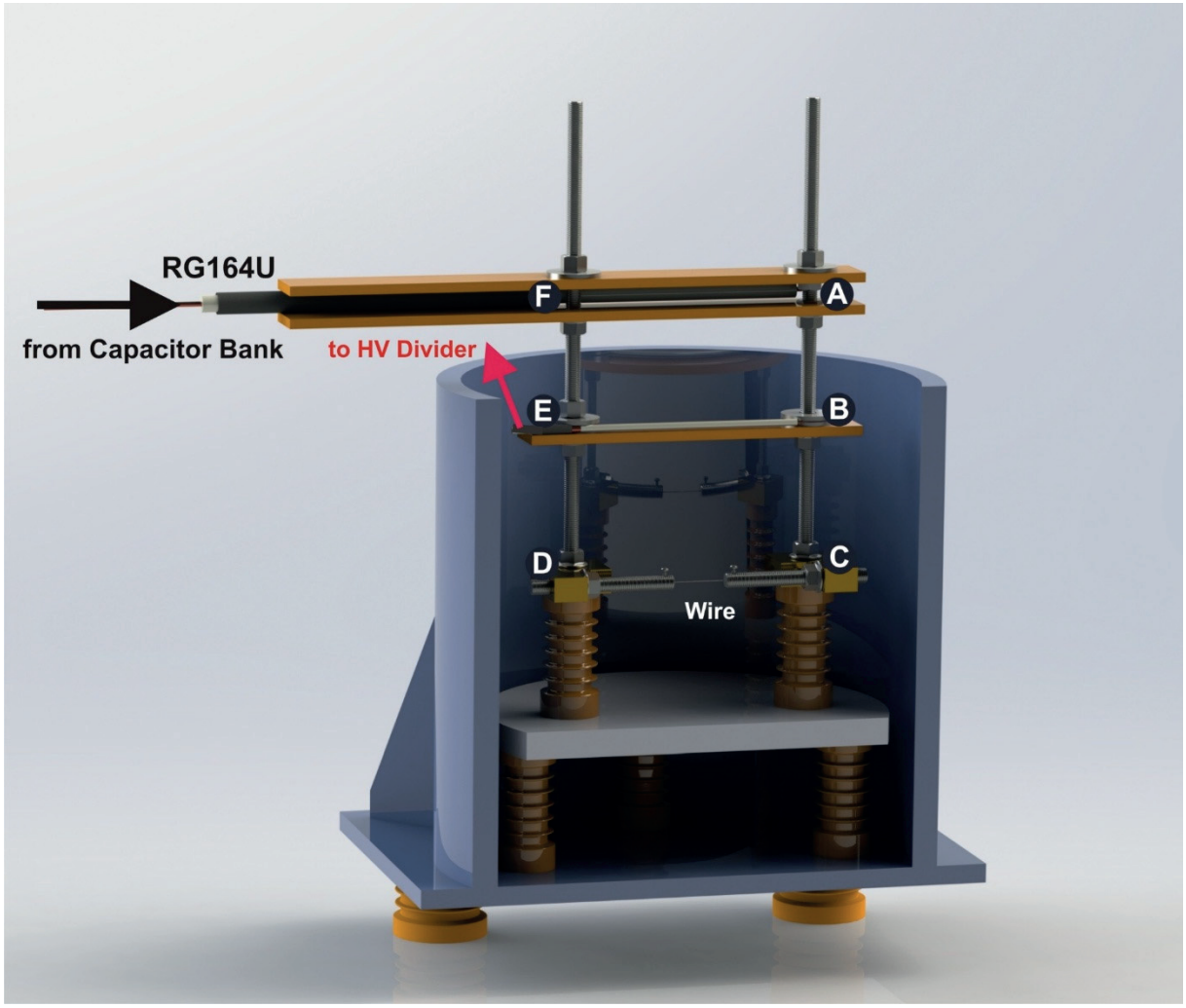

Fig. 11: CAD model of the clamp device inside the discharge chamber (geometric section)

3.2.3 The inductance of the clamp device

In order to be able to achieve an high increase of current dI/dt during the pulsed wire discharge experiments, the total value of inductance of the circuit should be low. As the inductance of the clamp device itself takes up a significant amount of the total circuit inductance, figuring out the specific amount is of special interest. By measuring the geometric dimensions of the clamp device (Fig. 11) a circuit model in regards to inductance was possible to be drawn (Fig. 12). According to Jackson [10] the inductance of a straight wire with the length l and a radius r is able to be calculated with the following formula:

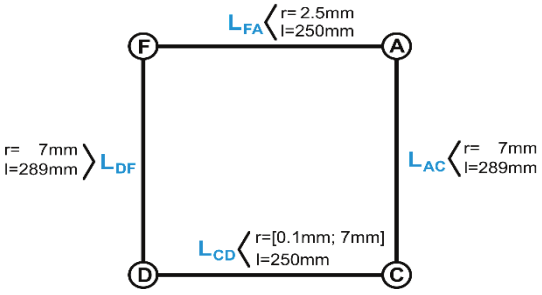

Fig. 12: Inductance model of the clamp device

$$L = \frac{\mu_0 l}{2\pi} \cdot \left[\ln\left(\frac{2l}{r}\right) - \frac{3}{4}\right] \tag{3.1}$$

The mutual inductance M=L_{ij} of two paths of wire *i*, *j* can be determined by integrating Neumann´s formula [11]. In the special instance, that two wires are parallel concerning length *l* and distance *d,* Rosa and Grover [12] derived the mutual inductance as follows:

$$M = \frac{\mu_0}{2\pi} \cdot \left[l \cdot ln\frac{l + \sqrt{l^2 + d^2}}{d} - \sqrt{l^2 + d^2} + d\right] \tag{3.2}$$

The inductance matrix of the system given in Fig. 12 is:

$$\hat{L} = \begin{pmatrix} L_{AC,AC} & L_{AC,CD} & L_{AC,DF} & L_{AC,FA} \\ L_{CD,AC} & L_{CD,CD} & L_{CD,DF} & L_{CD,FA} \\ L_{DF,AC} & L_{DF,CD} & L_{DF,DF} & L_{DF,FA} \\ L_{FA,AC} & L_{FA,CD} & L_{FA,DF} & L_{FA,FA} \end{pmatrix} . \tag{3.3}$$

By combining the two equations (3.1) and (3.2) with one another and also taking the geometric values given in Fig. 12 into consideration one receives the following:

$$\hat{L} = \begin{pmatrix} 211.76 & 0 & -30.65 & 0 \\ 0 & [388.36; 175.93] & 0 & -20.51 \\ -30.65 & 0 & 211.76 & 0 \\ 0 & -20.51 & 0 & 227.42 \end{pmatrix} nH$$

The sum of all the elements throughout the matrix, provides the specific value of inductance when a wire of the length l=250mm and radius r_{wire}=0.1mm is used, concerning the clamp device:

$$L_{clamp\ device}(r_{wire} = 0.1mm) = \sum_{ij} L_{ij} \approx 937nH$$

When a wire of the length l=250mm and radius r_{wire}=7mm is used, it functions in the same way as a short circuit with a threaded rod does instead of the wire. The inductance then becomes:

$$L_{clamp\ device}(r_{wire} = 7mm) = \sum_{ij} L_{ij} \approx 725nH$$

Hence, the maximum deviation of the value of inductance, which is caused by the geometry of the implemented wire, is determined with the following calculation: ΔL =937nH-725nH=212nH. This effect should be taken into account, when analysing the data from experiments in future.

3.3 The setup in order to measure discharges

3.3.1 The measurement of voltage

During the procedure of charging up the capacitor bank, the voltage of these capacitors is measured by a high voltage probe (VOLTCRAFT H 40) at a ratio of 1000:1 and with a 10MΩ multimeter (Fig. 13). With this configuration the charge voltage is able to be adjusted up to an accuracy of approximately 10V.

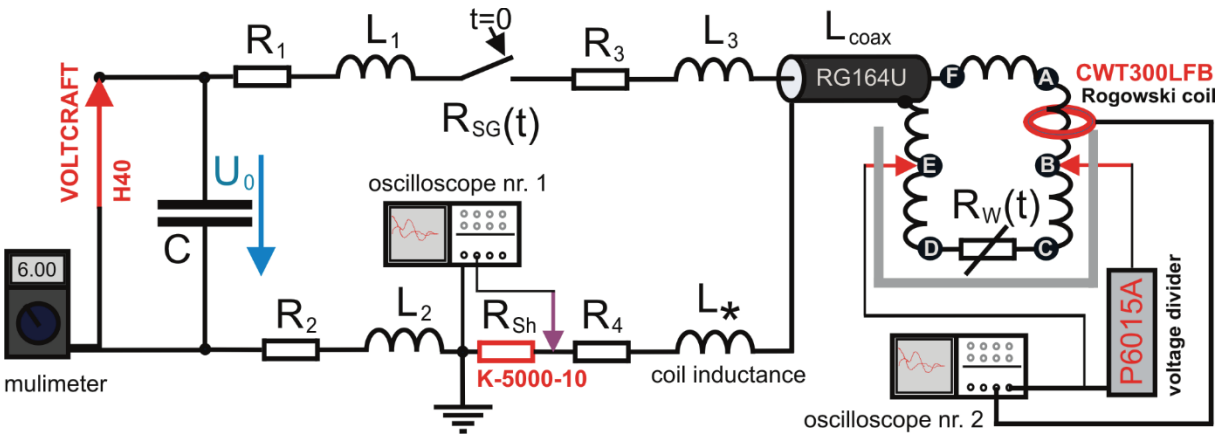

Fig. 13: Schematic of the setup required for discharge measurements

The main interest of this project are the discharge measurements, which display the characteristics of the exploding wires, so to be precise the decline in voltage throughout the wire resp. the wires plasma is measured by a high voltage probe from Tektronix (P6015A). Due to geometric limitations, it is not possible to measure the voltage directly from the relevant wire itself. Since the voltage is taped at the points Ⓑ and Ⓔ by a RG213U coaxial cable (Fig. 11, Fig. 13), the voltage U_{BE} is not exactly the same voltage as is U_{CD}. So as to be able to estimate this voltage difference one has to determine the inductance of the bridge circuit. The voltage U_{BE} is capable of being found out with the following formula:

$$U_{BE}(t) = (R_{BC} + R_{CD}(t) + R_{DE})I(t) + \left(L_{BC} + L_{CD} + L_{DE} - 2L_{BC,DE}\right)\frac{dI(t)}{dt} \qquad (3.4)$$

If one ignores R_{BC} and R_{DE} this formula occurs:

$$U_{BE}(t) = R_{CD}(t)I(t) + L_{clamp}\frac{dI(t)}{dt}\ . \qquad (3.5)$$

The value for L_{clamp} is calculable with the equations (3.1) and (3.2). By incorporating the geometric values from Fig. 11 one is able to gauge the existing inductance:

$$L_{clamp} = L_{BC} + L_{CD} + L_{DE} - 2L_{BC,DE} = 97nH + (282 \pm 106)nH + 97nH - 2 \cdot 10nH \approx (456 \pm 106)nH$$

When one assumes a total circuit inductance of 4.5µH the current rise at t=0µs is able to be approximated by:

$$\left.\frac{dI(t)}{dt}\right|_{t=0} = \frac{U_C(t=0)}{L_{circuit}} = \frac{6kV}{4.5\mu} \approx 1.33kA/\mu s$$

If an inductance of L_{clamp}= 456nH is given, then the maximum voltage error is determined by:

$$\Delta U_{max} = L_{clamp}\left(\frac{dI}{dt}\right)_{max} = 0.456\mu H \cdot 1.33kA/\mu s \approx 606V$$

In previous tests with the aforementioned high voltage probe (P6015A), significant values of RF-noise were determined, when the probe is in close proximity to high current setups (I>10kA), which made it quite difficult to attain usable measurements. In order to be able to overcome this challenge, it was necessary to manufacture a shield (Fig. 14a) for the high voltage probe (Fig. 15a, b). The low voltage output from the voltage divider is attached to a battery-driven oscilloscope from RIGOL (DS1054). This oscilloscope with four channels is placed inside a shielding steel box (Fig. 14b), isolators separate it from the floor.

Fig. 14a: Production process with a milling machine

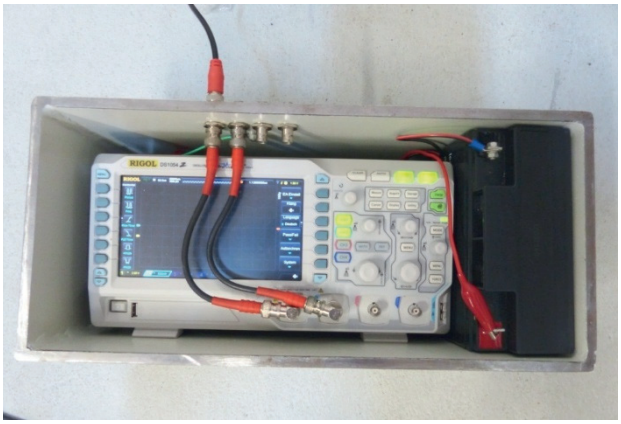

Fig. 14b: Battery powered oscilloscope inside shielding box

Fig. 15a: CAD-model - a section of the high voltage divider
① HV probe Tektronix P6015A
② turned part made of POM as attachment
③ Isolation made of acrylic glass
④ housing made of S235JR steel
⑤ HV feed through with RG213U coaxial cable

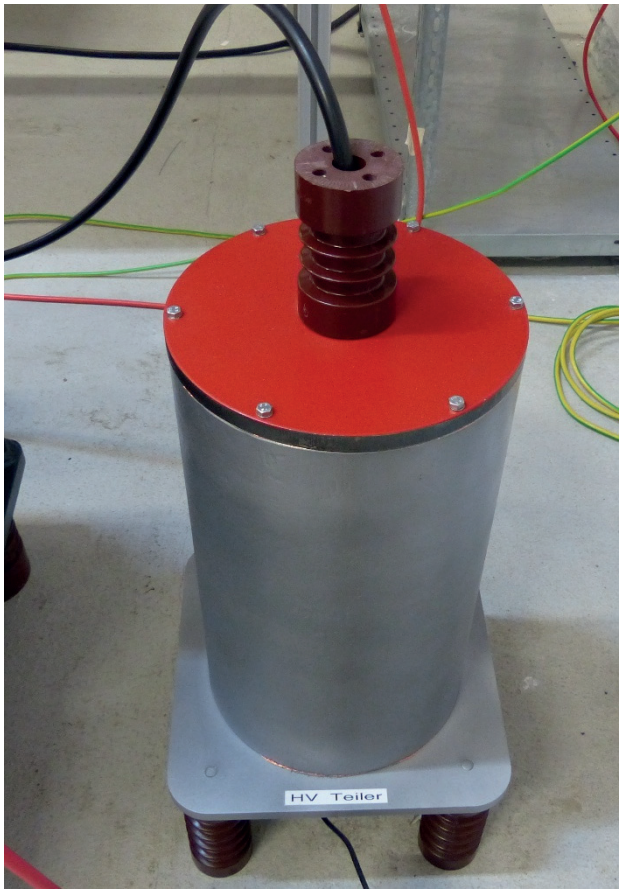

Fig. 15b: Practical realisation of the high voltage divider

3.3.2 The procedure of current measurements

After triggering the discharge of the capacitor bank, the given discharge current is measured by a high current coaxial shunt resistor (Fig. 16a) from the manufacturer T&M RESEARCH PRODUCTS, Inc. (K-5000-10). As a second option the discharge current can also be measured by a Rogowski coil (CWT 300LFB- 0.1mV/A), which is placed around one of the current-carrying threaded rods within the discharge chamber (Fig. 16b). Both measurement devices have a BNC output and therefore it is possible to connect them to the digital storage scope (Owon DS6062), which is used in order to be to able capture current curves while pulse discharges take place. This scope is also placed in a shielding steel box (S235JR), which is electrically isolated from the ground by high voltage isolators (Fig. 17a).

A comparison of the two types of measurement resulted in a perfect overlap of the current curves (Fig. 17b). No matter how one positions the Rogowski coil around the threaded rode (in one instance around the current-carrying threaded rod in the center, in another case touching the current-carrying threaded rod) one is unable to determine significant differences in comparison to measurements made with the coaxial shunt resistor. However the positioning of the Rogowksi coil seems to be even less critical than as it is mentioned within the producers manual [13].

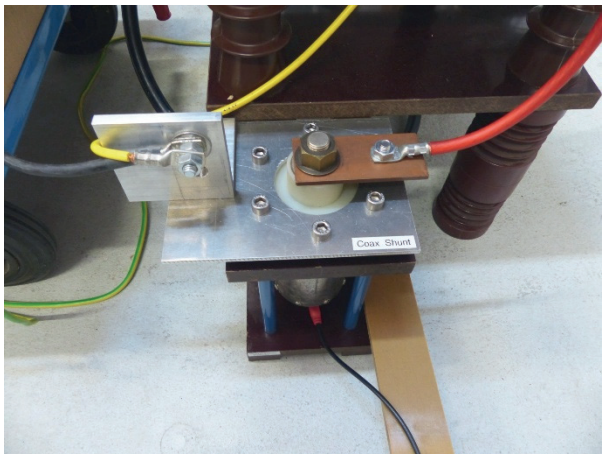

Fig. 16a: Coaxial shunt resistor

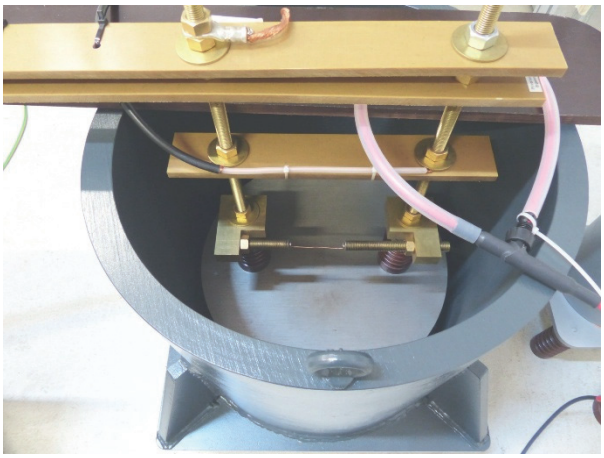

Fig. 16b: Rogowski coil (red loop around the threaded rod)

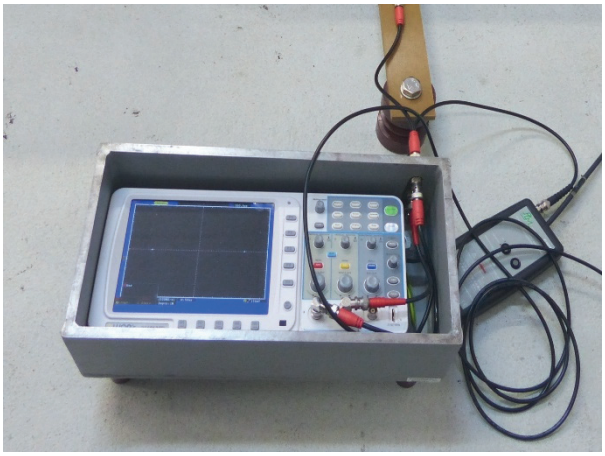

Fig. 17a: battery powered digital oscilloscop inside a shielded box (Owon DS6062)

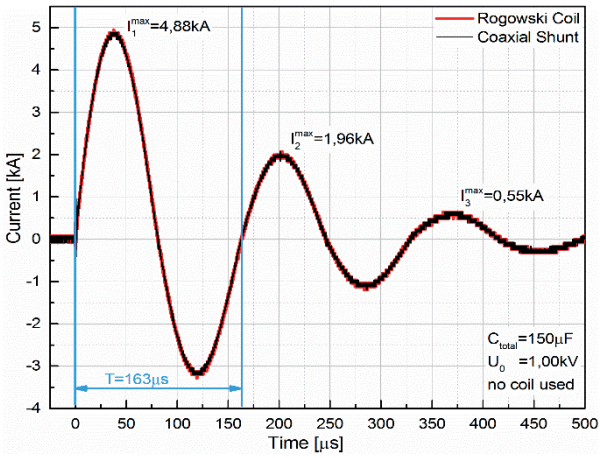

Fig. 17b: a comparison of current measurements

4. The results of the experiments

4.1 The evaluation of the circuit inductance

4.1.1 Measurements made with an impedance analyser

By using an impedance analyser it was possible to determine the resonance frequency of the capacitor bank network including the discharge circuit. When no coil was used within the circuit, the resonance frequency was measured at 6206Hz (Fig. 18). By installing a coil with an inductance L*≈4.1µH (see Fig. 13), the resulting resonance frequency was at a lower value of 4462Hz.

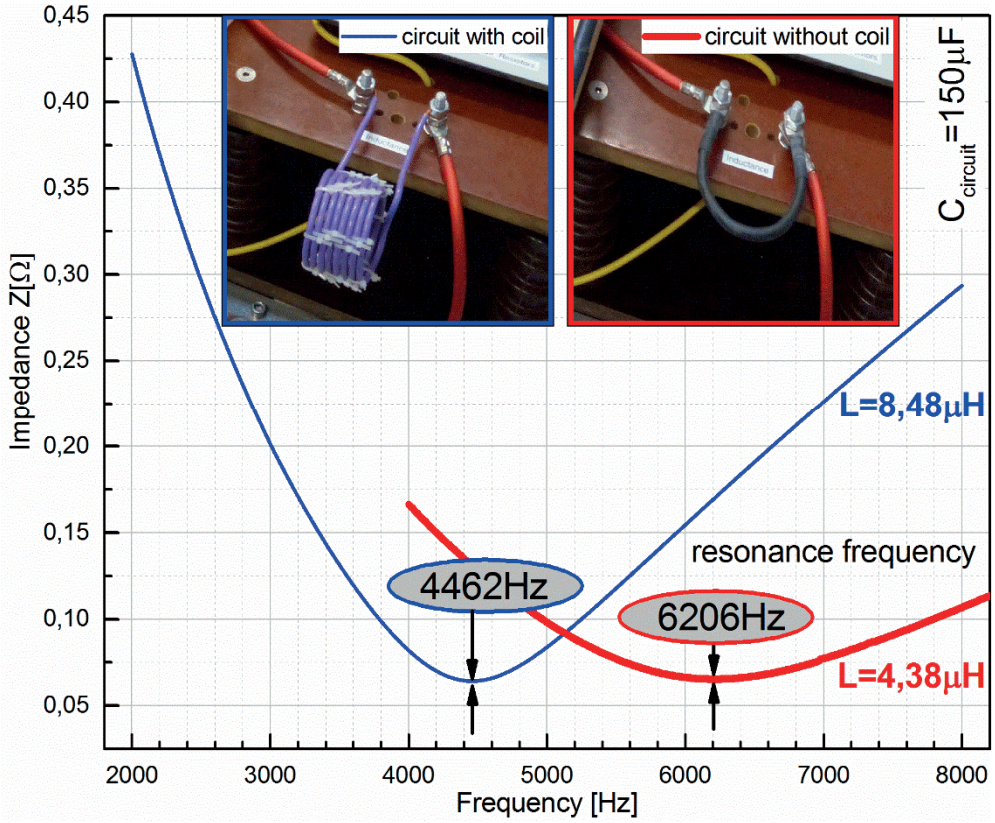

Fig. 18: The characteristic of impedance from the capacitor bank network

The total capacitance of the capacitor bank was measured with an LCR meter, which showed a value of $C_{circuit}$=(150±2)µF. By ignoring damping effects, the circuits inductance is able to be approximated by the Thomson equation:

$$L = \frac{1}{4\pi^2 f_0^2 C} \qquad (4.1)$$

Taking the two circuits into consideration one receives an inductance value of:

$$L(without\ coil) = \frac{1}{4\pi^2 (6206Hz)^2 150 \cdot 10^{-6} F} = 4.38uH.$$

$$L(with\ coil) = \frac{1}{4\pi^2 (4462Hz)^2 150 \cdot 10^{-6} F} = 8.48uH.$$

4.1.2 Shortcut discharges with low voltage

After short circuiting the electrodes inside the plasma chamber, the capacitor bank was charged up to a voltage of 1000V, which is equivalent to 75J (Fig. 7) of stored energy. In practical terms the inductance can be determined via the analysis of the low voltage bypass discharge oscillations within the given circle (Fig. 19a, b).

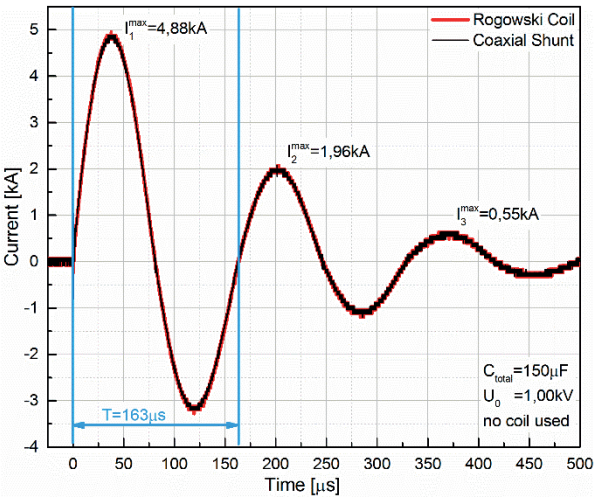

Fig. 19a: discharge current without a coil

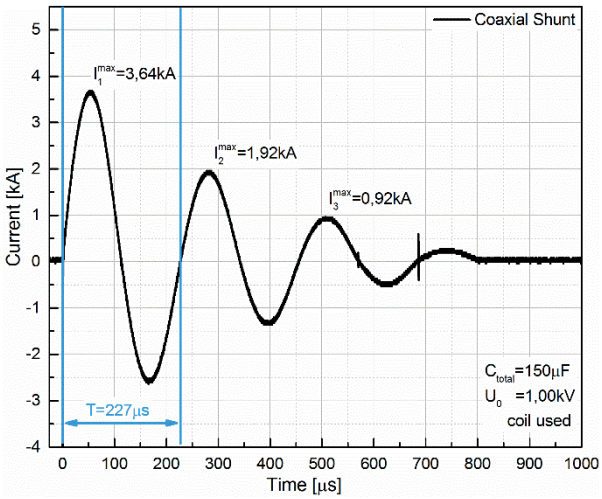

Fig. 19b: discharge current with a coil

The averaged logarithmic decrement $\overline{\Lambda}$ is able to be determined from n current maxima I^i_{max} with the same algebraic sign:

$$\bar{\Lambda} = \frac{1}{n}\sum_{i=1}^{n} \ln\left(\frac{I_{\max}^{\,i}(t)}{I_{\max}^{\,i+1}(t+T)}\right). \tag{4.2}$$

After incorporating the result into

$$L = \frac{T^2}{\left(4\pi^2 + \Lambda^2\right)\cdot C} \tag{4.3}$$

one receives a relatively accurate value concerning the equivalent circuit inductance. For the experimental setup with no coil the Inductance is:

$$L(without\ coil) = \frac{(163\mu s)^2}{(4\pi^2 + \left[\frac{1}{2}\left(ln\left(\frac{4.88}{1.96}\right) + ln\left(\frac{1.96}{0.55}\right)\right)\right]^2 \cdot 150\mu F} \approx 4.35\mu H$$

In the second instance concerning a coil usage, the value of inductance for the entire circuit is:

$$L(with\ coil) = \frac{(227\mu s)^2}{(4\pi^2 + \left[\frac{1}{2}\left(ln\left(\frac{3.64}{1.92}\right) + ln\left(\frac{1.92}{0.92}\right)\right)\right]^2 \cdot 150\mu F} \approx 8.59\mu H.$$

With a deviation of less than 2% both results relatively accurately confirm the previous measurements made with the frequency analyser (compare chapter 4.1.1).

4.1.3 The determination of an equivalent circuit diagram

By analysing the discharge diagrams as well as current measurements one is capable of designing a circuit diagram which also incorporates the inductance values of the bussbars (Fig. 20).

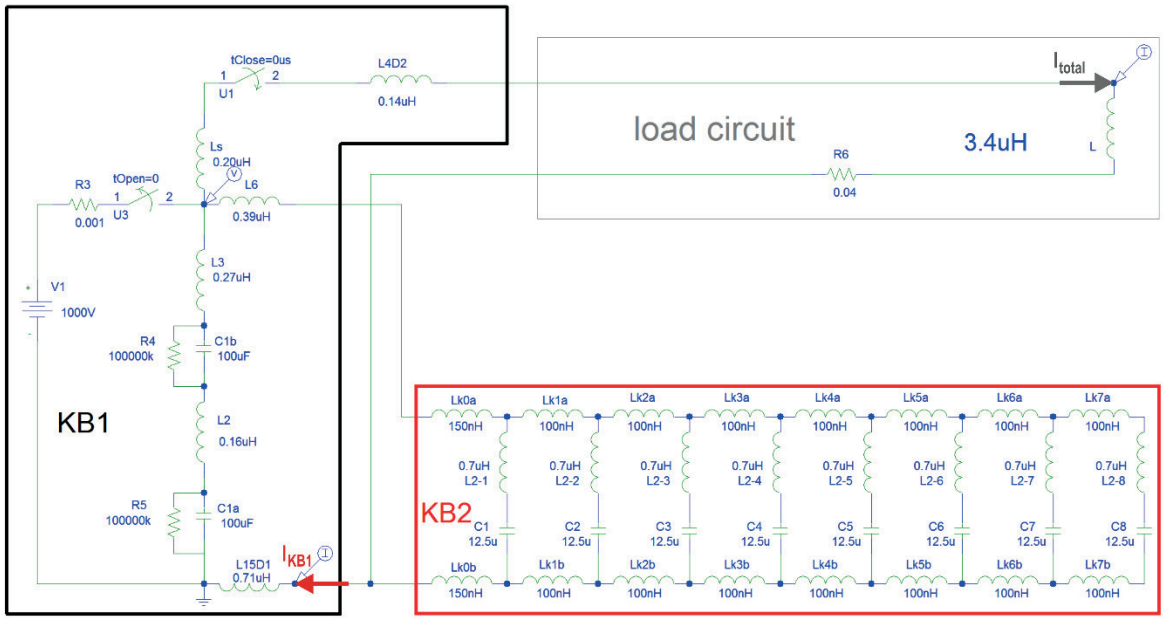

Fig. 20: A circuit diagram of the experimental setup. *The main capacitor bank KB1 (50µF) is connected in parallel to the additional capacitor bank KB2 (100µF). The whole capacitor bank has a capacitance of 150µF at a max. charge voltage of 6kV.*

Within Spice the designed circuit model of the capacitor bank was simulated. Variations regarding the utilised inductances produced a qualitative overlap compared with discharge measurements (Fig. 21).

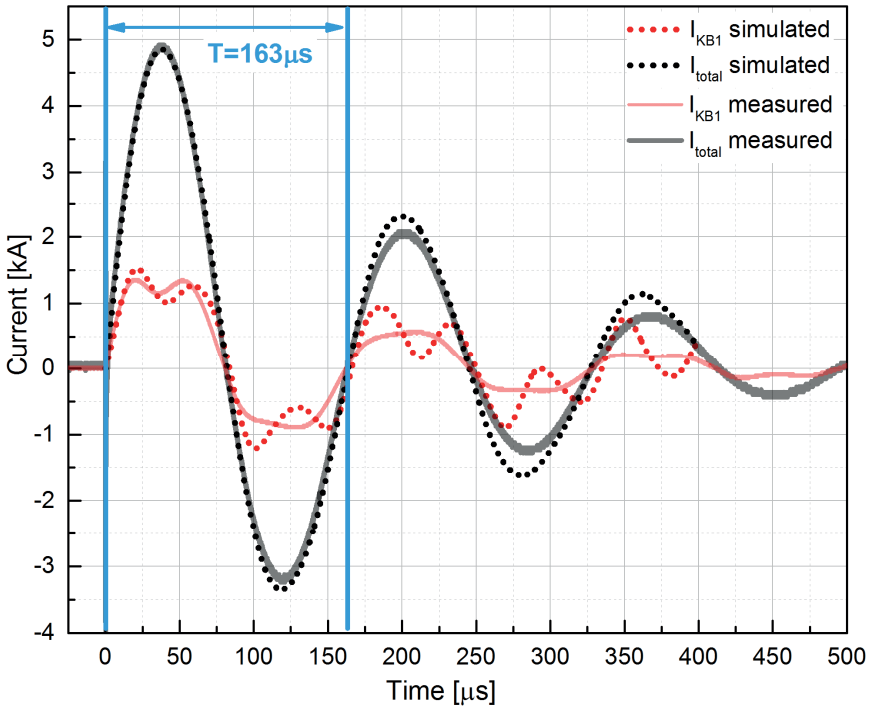

Fig. 21: Discharge current of the capacitor bank network. *Solid lines represent measured values, dotted lines represent simulated values.*

4.2 The discharge of a steel wire mid air

4.2.1 The voltage and current measurements

In a primary experiment a steel wire (X12CrNi18-8/ 1.4300) was fastened between the two electrodes inside the discharge chamber (Fig. 11). With a diameter of 820µm and a length of 80mm the used wire had a volume of $V = r^2\pi l = (410 \cdot 10^{-3}mm)^2 \cdot \pi \cdot 80mm \approx 42mm^3$. In accordance with the density of steel, the wire has a mass of approx. $m = \rho V = 7.9mg/mm^3 \cdot 42mm^3 \approx 332mg$. If one assumes that the vaporisation energy is 6.26kJ/g, then the required energy in order to vaporise the metal is:

$$E_{vap} = 6260\text{J/g} \cdot 0.332\text{g} \approx 2078\text{J}$$

At a voltage of 6kV the stored energy within the capacitor bank lies at $E_C = \frac{1}{2}CU^2 = \frac{1}{2}150 \cdot 10^{-6}F(6000V)^2 = 2700J$, which is around 622J more energy than is actually needed for total vaporisation. After charging up the capacitor bank the steel wire was able to be vaporised including a load bang. With the oscilloscope nr. 2 the voltage of the wire as well as the discharge current was captured (Fig. 22).

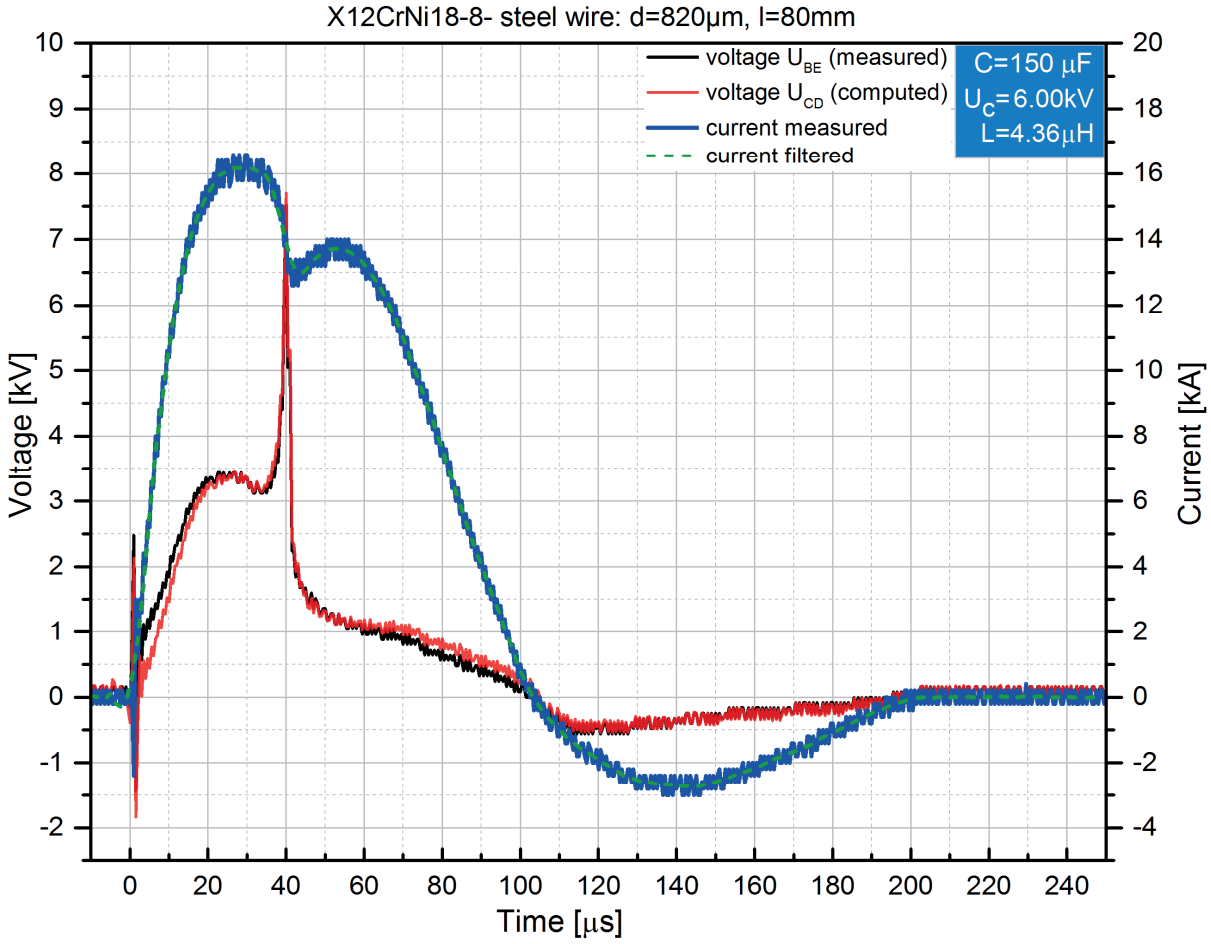

Fig. 22: The voltage and current measurement of a pulse discharge through a X12CrNi18-8 steel wire. *The given wire had a diameter of 820µm and a length of 80mm. The voltage U_{BE} is measured at the points Ⓑ and Ⓔ (see Fig. 11, Fig. 13) and rises to a maximum of around 3.4kV in 25µs. By using the equation (3.5) the voltage U_{DE} was corrected numerically by assuming L_{clamp}=456nH, which provided the curve voltage U_{CD}. The current reaches a total maximum of around 16kA after 30µs and decreases afterwards to 13kA. The plasma discharge starts at around 39µs and reaches a maximum at approximately 13.6kA.*

4.2.2 The power and energy absorption within wire and the wire plasma

The electrical power during the wire discharge is able to be calculated via simple multiplication of the voltage and current curve:

$$P_w(t) = U_W(t) \cdot I_W(t) \tag{4.4}$$

Fig. 23 shows the power of the wire discharge dependent on time.

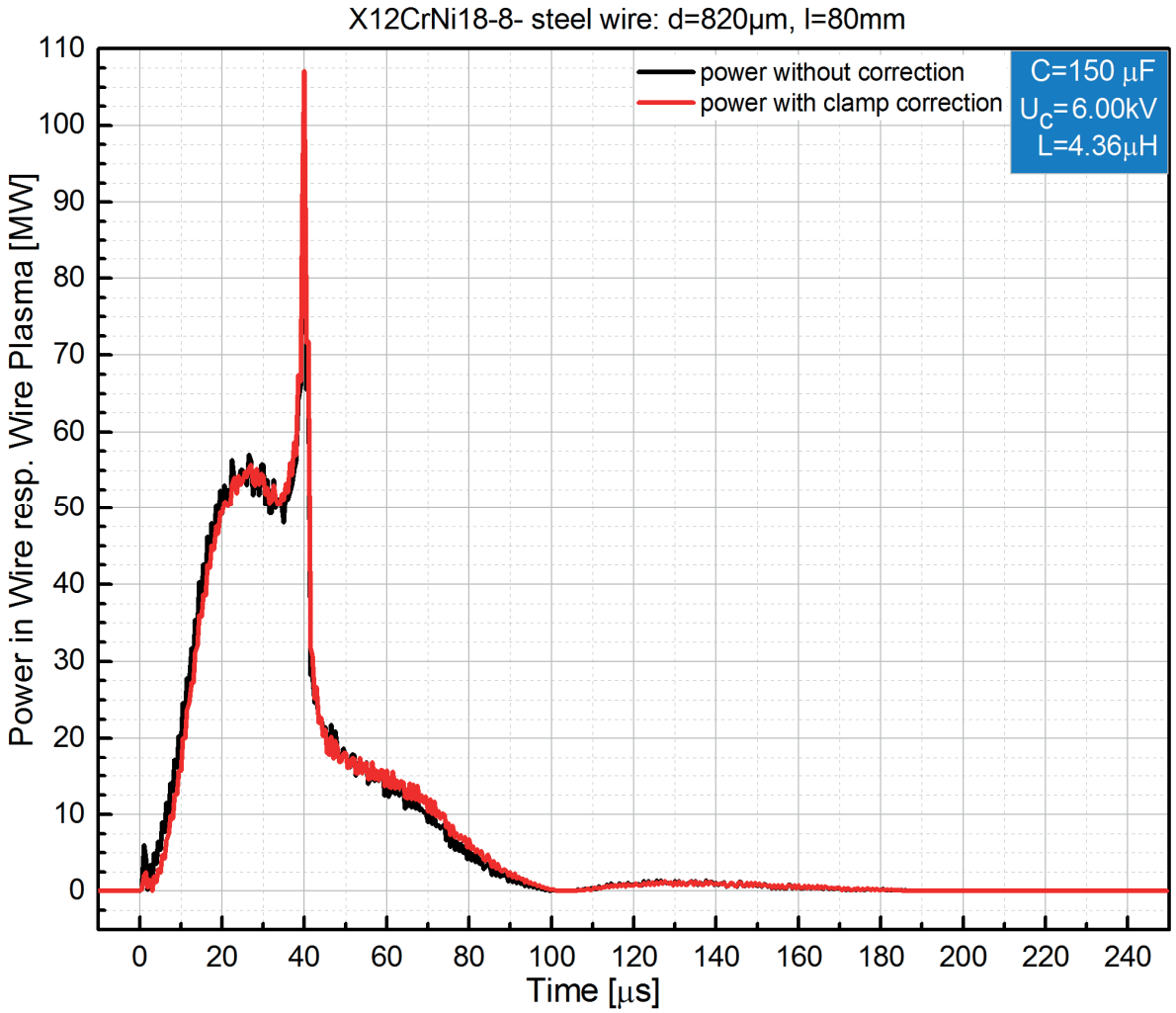

Fig. 23: The power curve during the pulsed wire discharge. *The curves "power without correction" and "power with clamp correction" deviate from one other to the order of approximately 18% at 70µs.*

The power curve reaches a primary maximum of around 53MW after 25µs. Straight after a brief dip down to 50MW occurs. At around 40µs a power value of approximately 107MW is reached. Through numerical integration of the power curve the absorbed energy within the wire resp. the wire plasma is able to be computed with:

$$E_W(t) = \int_0^t P(t)dt. \tag{4.5}$$

After numerical integration of the equation (4.5) the curve which represents the absorbed energy within the steel wire resp. the wire plasma was able to be plotted (Fig. 24).

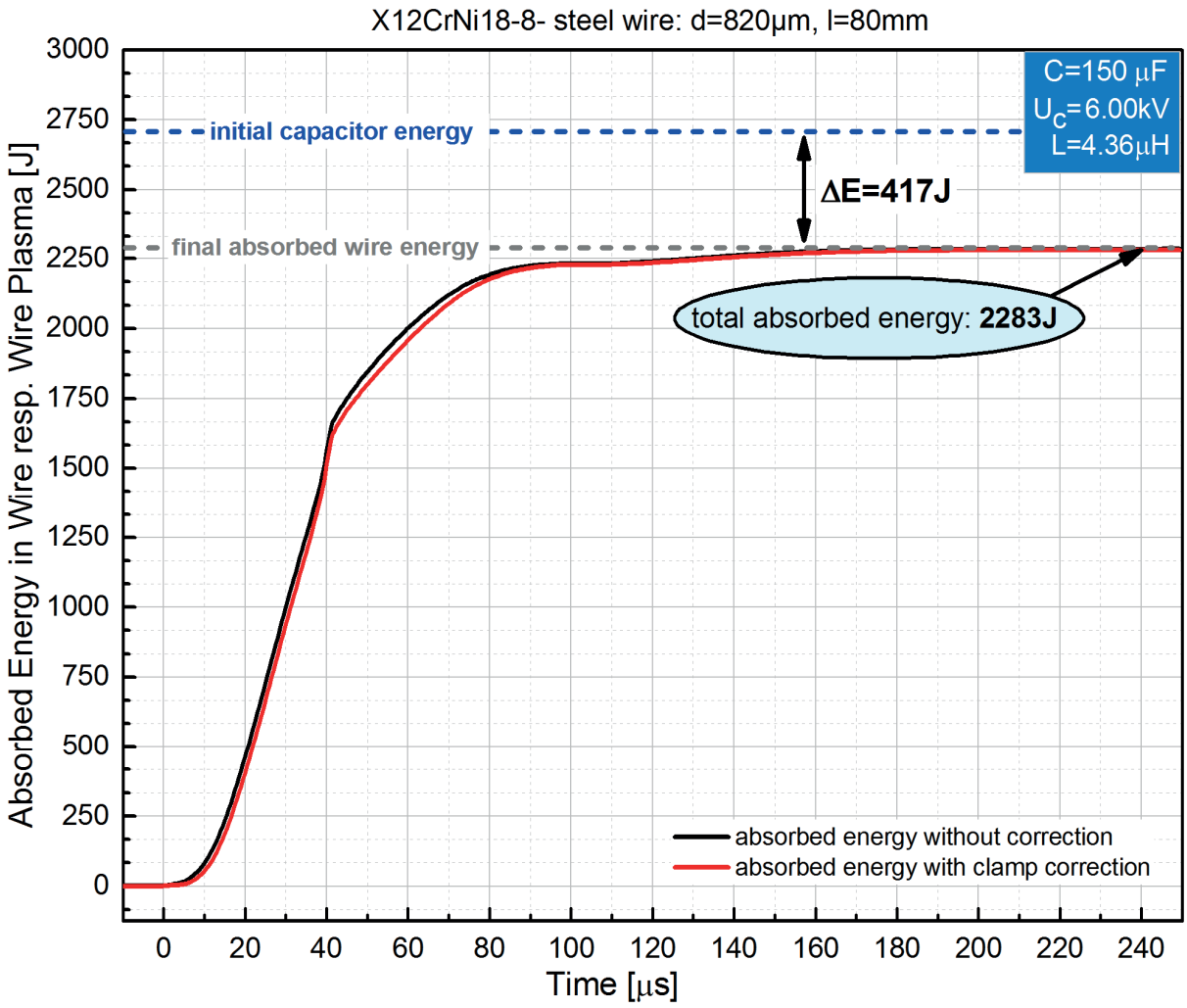

Fig. 24: The absorbed energy within the steel wire during the pulse discharge. *Between 10µs and 40µs the energy within the wire is nearly absorbed in a linear fashion and reaches a value of around 1500J. After 250µs a total energy of 2283J is absorbed by the wire resp. the wire plasma. The deviation of the absorbed energy with a correction (red curve) and without (black curve) reaches its maximum at around 60µs and differs in this case by approximately 2.5% from one another.*

Through numerical computation of the action integral

$$A(t) = \int_0^t I^2(t)dt \tag{4.6}$$

over long periods of time, a value of A(t→∞)=14034A^2s can be obtained. With a given start energy of 2700J the energy loss within the circuit lies at:

$$\Delta E = E_c(t=0) - E_W(t\to\infty) = 2700J - 2283J = 417J$$

Because the total energy in the system is

$$E_C(t=0) = \lim_{t\to\infty}\left[\int_0^t I^2(t)dt \cdot R_{circuit} + \int_0^t I^2(t)dt \cdot R_{wire}(t)dt\right], \tag{4.7}$$

one is capable of calculating the circuit resistance:

$$R_{circuit} = \frac{\Delta E}{A(t\to\infty)} = \frac{417J}{14034A^2s} \approx 30m\Omega$$

This value represents the averaged circuit resistance including the spark gap resistance.

5. The summary and discussion

This report describes the construction of an experimental setup in order to realise pulsed wire discharge experiments. The planning involved the personal construction of numerous special parts, which could not be purchased. Therefor a variety of pieces had to first of all be constructed in CAD and after that manufactured by utilising machine tools (a milling machine, a lathe and a welding machine). As the description of all these made parts would go far beyond the scope of this report, only the basic pieces and theoretical considerations where able to be presented. Nevertheless, a functioning experimental setup was able to be built, which allows pulsed wire discharges to be performed in order to generate shock waves in the air or under water. In a first experiment it was possible to demonstrate that the constructed setup is capable of explosive steel wire vaporisation. The captured waveform of the current and voltage represent a reliable measurement of the electrodynamic behavior during the pulsed discharge. The theoretical considerations regarding the inductance of the clamp device facilitated the correction of the measured voltage curve. Even though the determination of the clamp devices inductance value as 456nH appears to be rather appropriate, this value should be computated more accurately through FEM simulations.

Future experiments could also include a detailed analysis of the influence that wire dimensions have in regards to the specific characteristics of resistance which the chosen metal of the wire has. Experiments can be executed with standard conditions of atmosphere, in the air or underwater so as to be able to analyse the shock waves creation. By installing *Turmalin* pressure sensors inside the discharge chamber one is able to measure the dependency of shock wave creation related to the electrodynamic behavior during the explosion process of the used wire. By taking all these parameters into consideration it should be possible to discover a principal model for the resistance characteristics of the chosen wire. In future this model could be used for the simulation of arbitrary pulsed wire discharge experiments.

6. Literature

[1] Nairne, E: "*Electrical Experiments by Mr. Edward Nairne*", Phil. Trans. Roy. Soc. (London) 64, 79-89 (1774).

[2] Toepler, M.: "*Beobachtung von Metalldampfschichtung bei elektrischer Drahtzerstäubung*", Annalen *der* Physik 65, 873-876 (1898)

[3] McGrath: "*Exploding Wire Research 1774-1963",* Report from U.S. Naval Research Laboratory 1966

[4] Früngel F.: *"High Speed Pulse Technology, Vol. 1"*, Academic Press, New York 1965

[5] Lange, Kurt: "*Umformtechnik: Handbuch für Industrie und Wissenschaft*", Band 4, Springer Verlag, Berlin 1993

[6] General Atomics Energy Products: „*High Energy Density Capacitors for Pulsed Power Applications*", Engineering Bulletin, IEEE Pulsed Power Conference, July 2009

[7] Jäger H., Habilitationsschrift, Universität Kiel (1970).

[8] Tiemann W.: "*Über die gasdynamischen Vorgänge während der Dunkelpause von Drahtexplosionen und ihre Bedeutung für die Wiederzündung*", Z. Naturforsch. 23 a, 1952—1960 (1968)

[9] Philippow Eugen*: "Grundlagen der Elektrotechnik"*, Verlag Technik 1992

[10] Jackson John David: *"Classical Electrodynamics"*, De Gruyter, 3. Auflage 2002

[11] Neumann, F. E. *"Allgemeine Gesetze der inducirten elektrischen Ströme*", Abhandlungen der Königlichen Akademie der Wissenschaften zu Berlin, *1845. 143: 1–87*

[12] E. B. Rosa, F. W. Grover: "*Formulas and Tables for the Calculation of Mutual and Self-Inductance"*, Bulletin of the Bureau of Standards, Vol. 8, 1-287 (1912), Washington, 1907.

[13] *APPLICATION NOTES*, Power Electronic Measurements Ltd, http://www.pemuk.com/Userfiles/CWT/CWT%20-%20Technical%20notes%20-%20001.PDF (download from 16.8.2018)

Statutory Declaration

surname: Maximilian last name: Bigelmayr

matriculation number: 216206098 master course: Electrical Power Engineering

date of submission: 23.8.2018

Hereby I declare on oath, that I, Maximilian Bigelmayr, have authored independently this report with the title "*Construction of an Experimental Setup for Studies on Pulsed Wire Discharge Experiments*" and did not use any other means than indicated. The parts of the work which have been taken in the wording or meaning of other works are indicated in each case with naming of the original reference.

Signature: _____